Physical Insights into Solar Center-to-Limb RV Variability with SDO

PennState Eberly College of Science

Center for Exoplanets and Habitable Worlds

Michael L. Palumbo III[1], Steve Saar[2], Raphaëlle Haywood[3]

1. Center for Exoplanets and Habitable Worlds, Penn State University
2. Center for Astrophysics | Harvard & Smithsonian
3. University of Exeter

palumbo@psu.edu

michaelpalumbo.me

0. Background & Goals

Background: Intrinsic stellar variability produces RV noise exceeding 1 m/s in Sun-like stars, drowning the 10 cm/s signals expected for Earth-like planets.

Goal: Use data from the Solar Dynamics Observatory to probe the center-to-limb variations in velocities seen in different solar region types.

Importance: We need to understand the contribution of velocity flows, such as those seen in Evershed flows, etc., to properly model stellar RV variability.

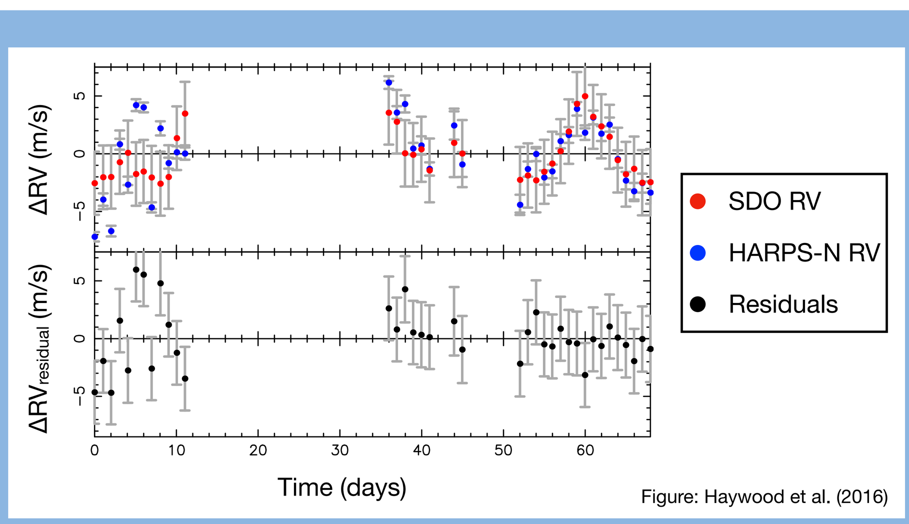

Figure: Haywood et al. (2016)

Previous works (Haywood et al. 2016, Milbourne et al. 2019, Ervin et al. 2022) have shown that RVs computed from Solar Dynamics Observatory (SDO) data strongly correlate with RVs from the HARPS-N and NEID spectrographs. But unlike these spectrographs, SDO spatially resolves the solar disk, enabling studies that correlate specific active regions and other surface inhomogeneities with apparent RV excursions.

1. Perform SDO Data Corrections

HMI Continuum

SDO/HMI continuum corrected for limb darkening

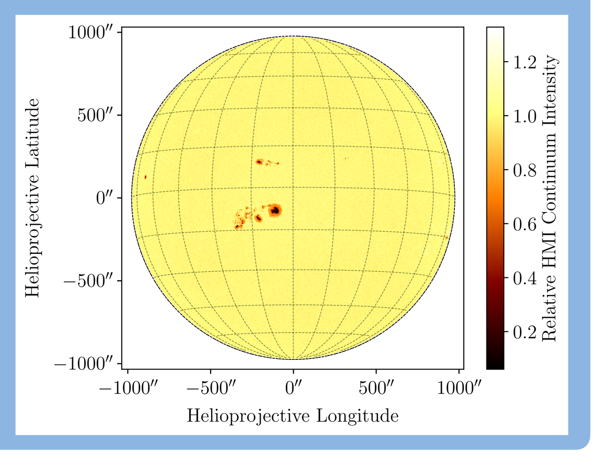

HMI Magnetogram

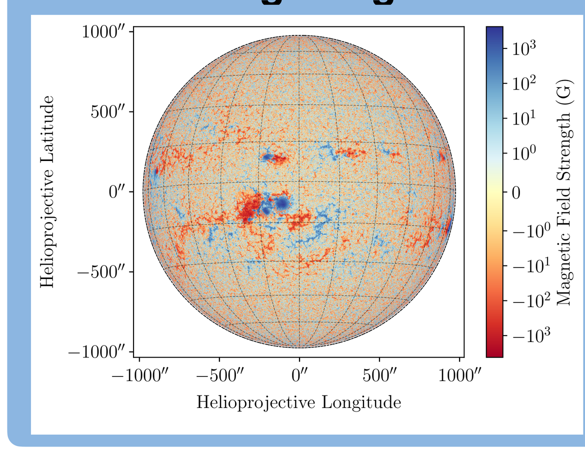

SDO/HMI magnetogram with foreshortening correction

HMI Dopplergram

SDO/HMI dopplergram corrected for differential rotation and observer velocity

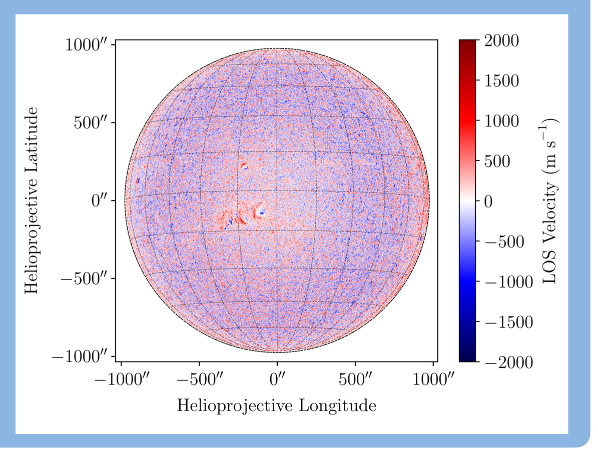

AIA 1700Å Continuum

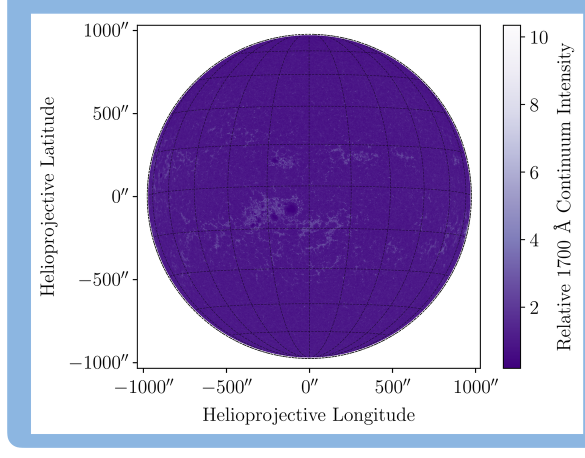

SDO/AIA 1700Å filter gram corrected for limb brightening

2. Use SDO/HMI + AIA Data to Classify Pixels

Classification Thresholds

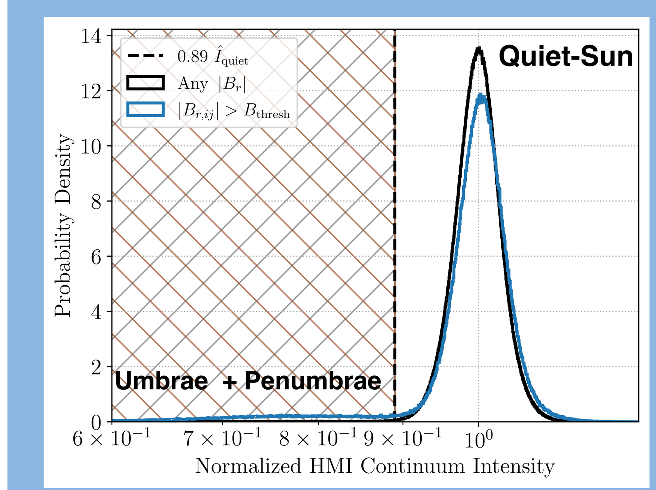

Distribution of continuum intensities with threshold from Yeo et al. (2013) used to separate quiet Sun from spots.

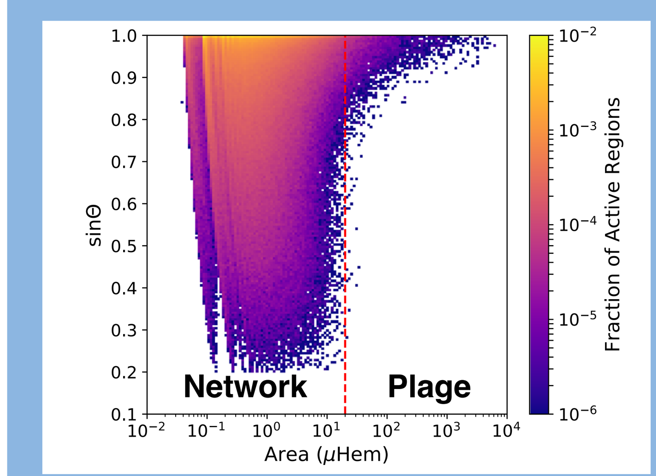

Distribution of bright region areas from Milbourne et al. (2019) with threshold used to separate large magnetic areas (plage) from small ones (network).

Figure: Milbourne et al. (2019)

The distributions of continuum intensities, magnetic field strengths, and region areas are used to construct thresholds used to classify regions. Our classifications thresholds are expanded from those first used in Yeo et al. (2013), Haywood et al. (2016), and Milbourne et al. (2019).

Pixel Classification Map

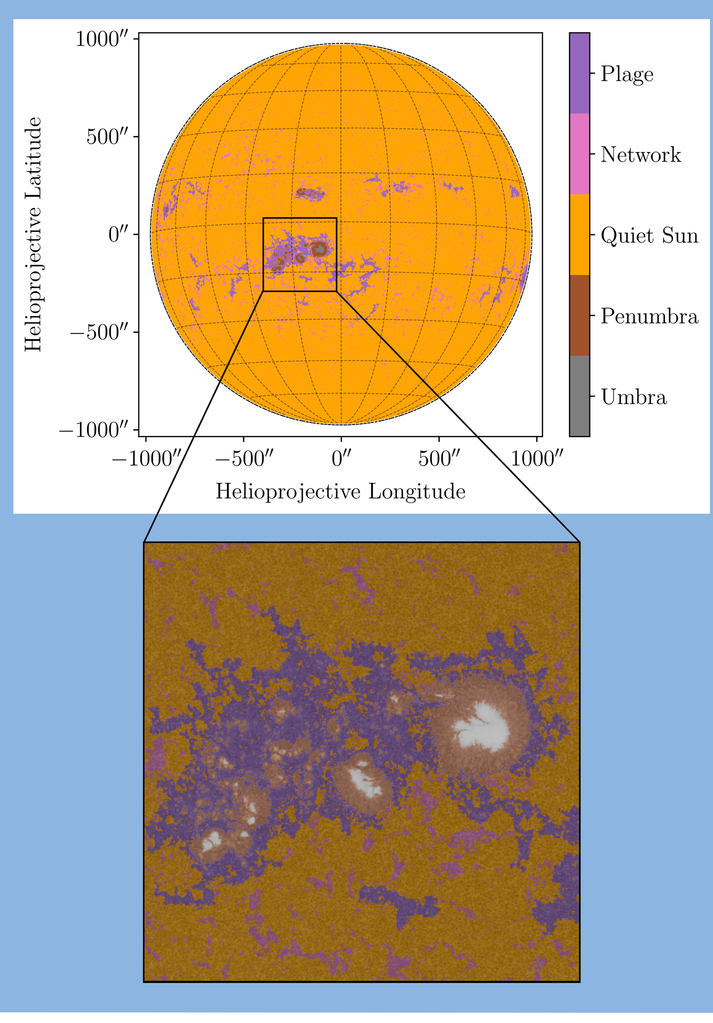

The thresholds are used to uniquely classify each pixel observed by SDO. Classifications are carried out for six observation epochs each day of 2012-2015. After classification we compute velocities in 10 radial bins, linear in μ.

3. Calculate velocities in μ bins

Total velocity

$$\hat{v} = \frac{\Sigma_{ij}\left(v_{ij} - \delta v_{sc,ij} - \delta v_{rot,ij}\right) I_{ij}}{\Sigma_{ij} I_{ij}}$$

The total velocity is the intensity-weighted sum of the HMI Dopplergram corrected for spacecraft motion and solar differential rotation.

Quiet-Sun velocity

$$\hat{v}_{\rm quiet} = \frac{\Sigma_{ij}\left(v_{ij} - \delta v_{sc,ij} - \delta v_{rot,ij}\right) I_{ij} W_{ij}}{\Sigma_{ij} I_{ij} W_{ij}}$$

The quiet-Sun velocity is the same as above, but only computed for pixels classified as quiet Sun.

Suppression of convective blueshift

$$\Delta\hat{v}_{\rm conv} = \hat{v} - \hat{v}_{\rm quiet}$$

The suppression of convective blueshift is the difference of the above velocities.

We compute each velocity for each region classification in 10 radial bins.

4. Construct center-to-limb velocity distributions

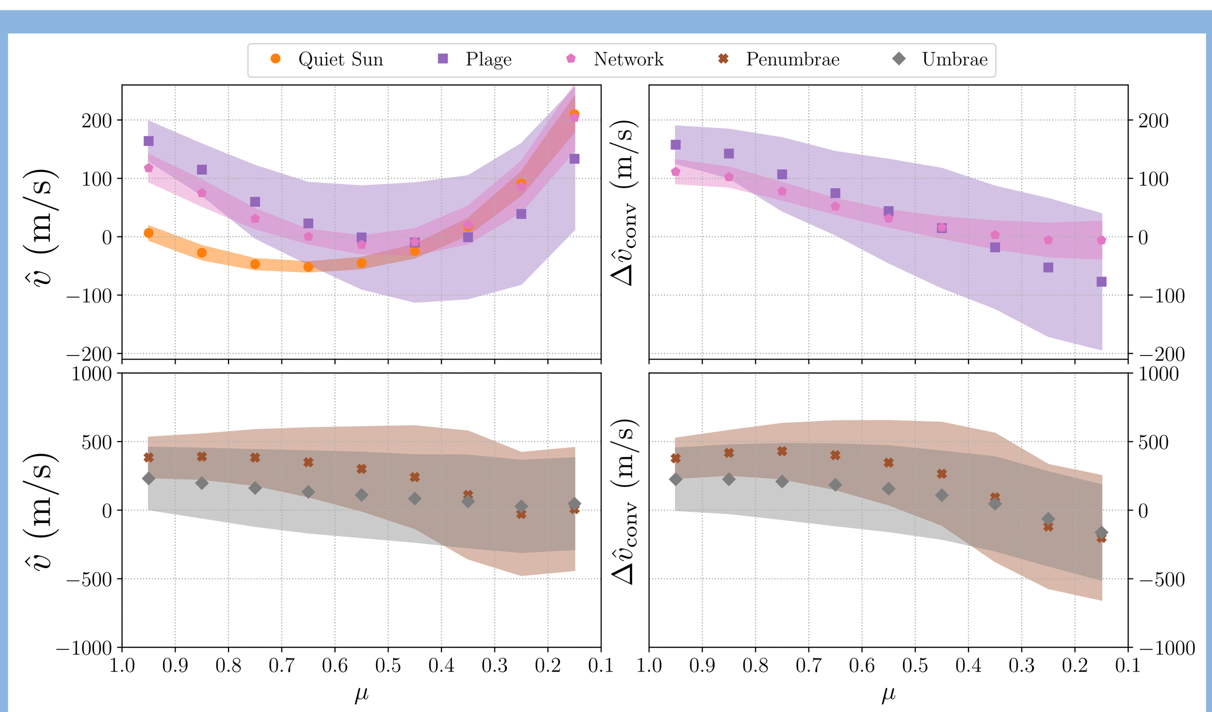

Center-to-limb velocity curves for each pixel classification, with the total velocity at left and the suppression of convective blueshift at right. Disk-center is at the left in each plot, and the limb at the right. The quiet-Sun curve shows the well-known convective blueshift variation. Notably, the plage and network curves show distinct variations, and the network curve approaches the quiet-Sun velocity distribution near the limb. The spread of velocities in umbrae and penumbrae are quite large compared to the other regions.

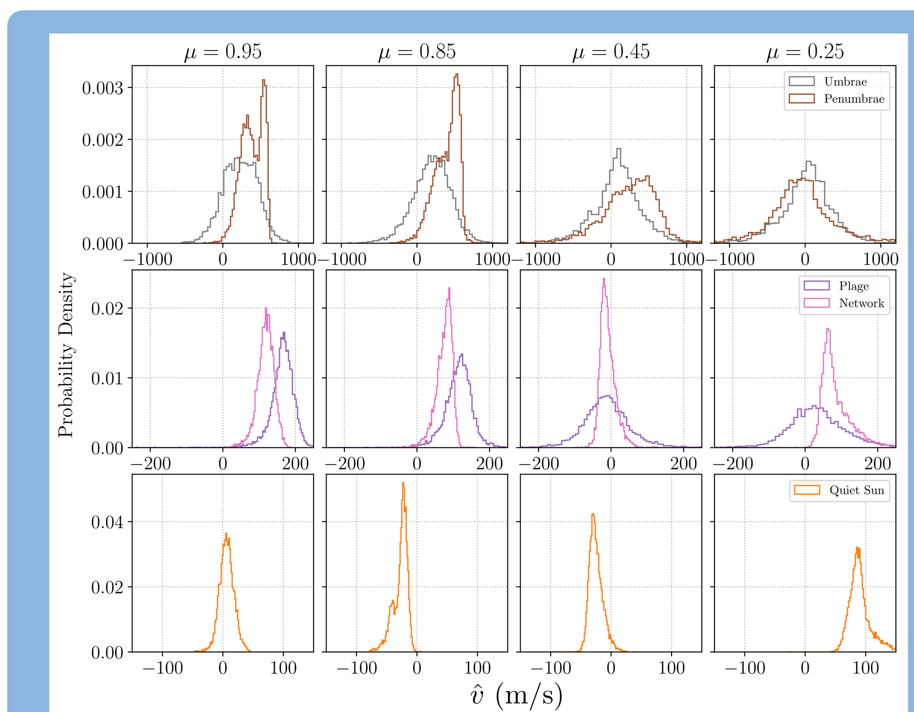

Full velocity distributions for a subset of μ bins. Bimodalities for certain pixel classifications in certain μ bins are evident. The widths of the plage velocity distributions increase with limb angle, whereas the network distributions remain relatively peaked. The quiet-Sun distribution develops a redshifted tail near the limb that is indicative of horizontal velocity flows near the tops of granules.

5. Takeaways

Penumbrae

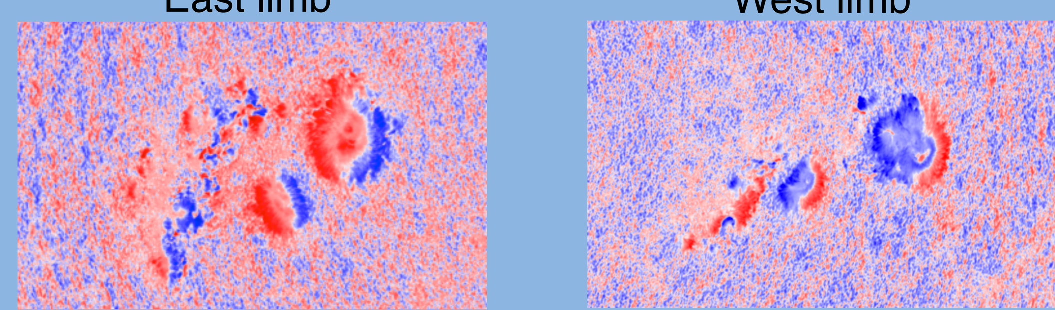

Strong velocity flows tangent to the solar surface are very sensitive to viewing angle. Future models of stellar variability should explore including these velocities as additional sources of radial velocity noise.

Plage + Network

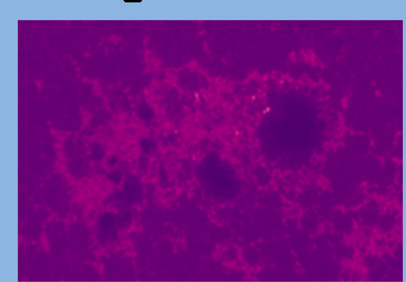

Plage and network exhibit distinct velocity distributions and may need to be modeled as separate noise components.

Quiet Sun

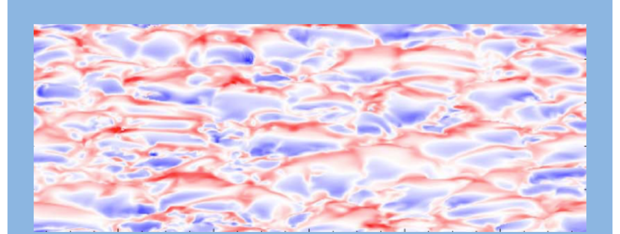

Figure: Cegla et al. (2018)

Near the limb, the corrugation of the solar surface by granulation produces a redshifted tail of velocities.

References

1. Haywood et al. (2016), MNRAS, 457, 4
2. Milbourne et al. (2019), ApJ, 874, 1, 107
3. Ervin et al. (2022), AJ, 163, 6, 272
4. Yeo et al. (2013), A&A, 550, A95
5. Cegla et al. (2018), ApJ, 886, 1, 55

Acknowledgments

SDO data products used in this work are provided courtesy of NASA/SDO and the AIA, EVE, and HMI science teams. M.L.P. acknowledges the support of the Penn State Academic Computing Fellowship. The Center for Exoplanets and Habitable Worlds is supported by the Pennsylvania State University and the Eberly College of Science. Computations for this research were performed on the Pennsylvania State University's Institute for Computational and Data Sciences' Roar supercomputer. S.H.S. gratefully acknowledges support by NASA EPRV grant 80NSSC21K1037, XRP grant 80NSSC21K0607, and Heliophysics LWS grant NNX16AB79G. R.D.H. is funded by the UK Science and Technology Facilities Council (STFC)'s Ernest Rutherford Fellowship (grant number ST/V004735/1).